

# Systematic Design of Electrothermomechanical Microactuators using Topology Optimization

O. Sigmund

Department of Solid Mechanics, Technical University of Denmark  
DK-2800 Lyngby, Denmark, sigmund@fam.dtu.dk

## ABSTRACT

Design methods for MicroElectroMechanical Systems (MEMS) have, until now, typically been based on intuition, experience and trial and error approaches. A method which may be used to design mechanical and electromechanical coupling parts of MEMS in a systematic way is the topology optimization method. In this paper, the method is applied to the design of electrothermomechanical microactuators.

The topology optimization method is a numerical procedure that distributes one or more passive or active materials in a design domain, such that some output performance is optimized. Here, the output work performed on a workpiece of given stiffness is to be maximized with a constraint on the minimum value of the resistance.

One example shows how an optimal actuator layout is dependent on geometry of the design domain and on the minimum allowable resistance of the device. Another example demonstrates the systematic design of an xy-scanning device with zero cross-sensitivity.

**Keywords:** Actuators, MicroElectroMechanical Systems (MEMS), Topology Optimization, Finite Element Analysis.

## INTRODUCTION

Manufacturing and processing techniques for MEMS have reached a high level of maturity and new devices can be built in a manner of days in labs and fundries. In contrast to that, modelling and especially development of *systematic* design methods is still in its infancy. Due to the lack of existing systematic design methods for MEMS, many devices are designed using intuition, experience and trial and error approaches. Furthermore, many devices are build from rectangular sub-elements ordered in "Manhattan"-like horizontal/vertical grids. Obviously, systematic design methods should be able to improve existing designs considerably and come up with entirely new or more efficient devices. Until now, however, no methods have been able to predict better designs of MEMS.

A promising method which may be able to solve some of above mentioned problem is the *topology optimization*

*method*. The topology optimization method [1], [2] was originally developed for large scale structural design problems and is an iterative numerical method consisting of alternating finite element analyses, sensitivity analyses and material redistribution. The topology optimization method solves the problem of distributing a given amount of material freely in a design domain such that some performance criterion is maximized.

This paper present an extension of previous works on design of *passive* MEMS [3]–[5]. In those works topology optimization was used to design micromanipulators which where operated using external probes. To allow for *on-chip* actuation, different actuation principles have been investigated. In [6] the method was applied to the design of thermomechanical actuators. This paper will deal with the principle of electrothermomechanical actuation. The electrothermal actuation principle is based on local resistive heating due to an applied electric field.

The paper is organized as follows. First, the governing equations for an electrothermomechanical system are formulated. Then, the design problem is defined and the computational procedure is briefly described. Several examples are given. First, it is shown how an existing design can be improved considerably and second, the method is applied to the systematic design of a xy-scanning device with two electrical inputs. Finally, a few words are devoted to the manufacturing process.

## MODELLING

The first step in the topology optimization procedure is to develop a model for the evaluation of the mechanical response of the microactuator subject to an applied electric field.

The structure to be analyzed is a sub domain of the domain  $\Omega$ . The boundaries are composed of six, pairwise disjoint regions  $\Gamma = \overline{\Gamma_{u_0}} \cup \overline{\Gamma_{t_0}} = \overline{\Gamma_{u_1}} \cup \overline{\Gamma_{t_1}} = \overline{\Gamma_{u_2}} \cup \overline{\Gamma_{t_2}}$  where the indices 0, 1 and 2 refer to electrical, thermal and elastic boundary conditions, respectively (see fig 1). Regions  $\Gamma_{u_i}$  can coincide, partly overlap or be fully disjoint, which holds for regions  $\Gamma_{t_i}$  as well. The domain  $\Omega$  contains a linear thermoelectroelastic material. Small displacements and constant material properties are assumed.

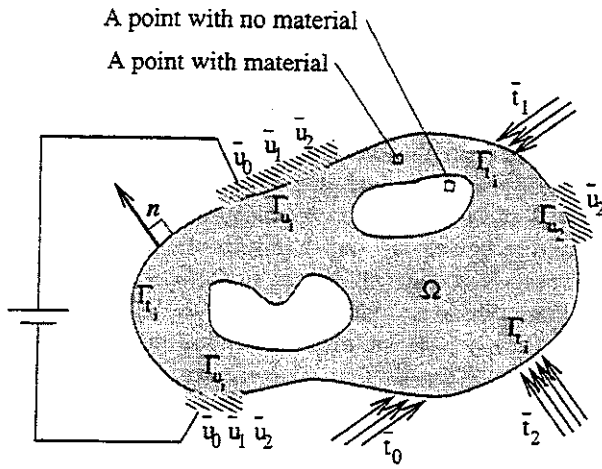


Figure 1: Loadings and boundary conditions for the general electrothermoelastic load problem.

The governing equations for, respectively, the electrical, the thermal and the elastic fields are

$$\left. \begin{aligned} \mathbf{k}_0 \nabla u_0 + \mathbf{b}_0 &= 0, & \text{in } \Omega \\ u_0 &= \bar{u}_0, & \text{on } \Gamma_{u_0} \\ \mathbf{n} \mathbf{k}_0 \nabla u_0 &= \bar{t}_0, & \text{on } \Gamma_{t_0} \end{aligned} \right\}, \quad (1)$$

$$\left. \begin{aligned} \mathbf{k}_1 \nabla u_1 + \mathbf{b}_1 &= 0, & \text{in } \Omega \\ \mathbf{b}_1 &= u_0 \mathbf{k}_0 \nabla u_0 & \\ u_1 &= \bar{u}_1, & \text{on } \Gamma_{u_1} \\ \mathbf{n} \mathbf{k}_1 \nabla u_1 &= \bar{t}_1, & \text{on } \Gamma_{t_1} \end{aligned} \right\}, \quad (2)$$

$$\left. \begin{aligned} \nabla \sigma + \mathbf{b}_2 &= 0, & \text{in } \Omega \\ \sigma &= \mathbf{E} (\epsilon(\mathbf{u}_2) - \alpha u_1), & \text{in } \Omega \\ \epsilon &= \frac{1}{2} [\nabla \mathbf{u}_2 + (\nabla \mathbf{u}_2)^T], & \text{in } \Omega \\ \mathbf{u}_2 &= \bar{\mathbf{u}}_2, & \text{on } \Gamma_{u_2} \\ \sigma \mathbf{n} &= \bar{\mathbf{t}}_2, & \text{on } \Gamma_{t_2} \end{aligned} \right\}, \quad (3)$$

where  $u_0$  is voltage,  $u_1$  is temperature change,  $u_2$  is the displacement vector,  $\mathbf{b}_0$  is the vector of prescribed internal current source per unit volume,  $\mathbf{b}_1$  is the vector of internal heat generation per unit volume,  $\mathbf{b}_2$  is the body force vector,  $\mathbf{k}_0$  and  $\mathbf{k}_1$  are the electrical and thermal conductivity matrices, respectively,  $\mathbf{E}$  is the elastic stiffness matrix,  $\bar{u}_0$  and  $\bar{u}_1$  are prescribed voltage and temperature, respectively,  $\bar{u}_2$  is the prescribed displacement vector,  $\bar{t}_0$  and  $\bar{t}_1$  are prescribed current and heat flux, respectively,  $\bar{t}_2$  is the traction vector,  $\epsilon$  and  $\sigma$  are the strain and stress vectors, respectively,  $\alpha$  is thermal expansion vector and  $\mathbf{n}$  is the unit normal vector to the surface  $\Gamma$ . Remark that the internal heat generation  $\mathbf{b}_1$  is a function of the electric current  $u_0$  and that the stress  $\sigma$  is a function of the temperature  $u_1$ .

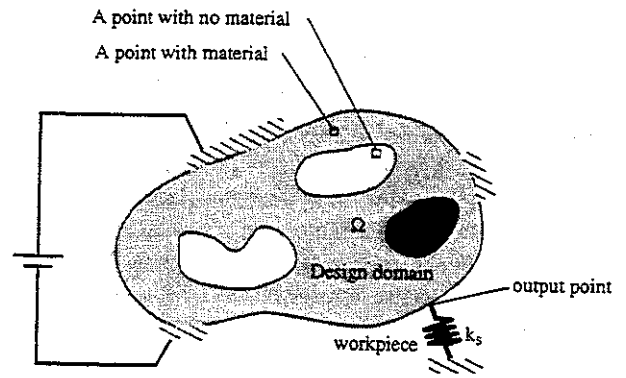


Figure 2: Design problem for electrothermal actuation.

## DESIGN PROBLEM

A design problem for electrothermal actuation is sketched in Fig. 2. The design problems consist in distributing a given amount of material in the planar design domain (grey area) such that the force exerted on a workpiece of given stiffness  $k_s$  is maximized. Some areas of the design domain may be restricted to be void (white areas) and some may be restricted to be solid material (black areas). The optimal actuator topology will depend on the stiffness of the workpiece. For a soft workpiece the actuator needs to displace a lot to build up a large force, whereas for a stiff workpiece a large output force does not require a large displacement. In this way, one can design force oriented or displacement oriented actuators by varying the stiffness of the workpiece as discussed in further details in [5] and [6].

The output force  $F_{out}$  exerted on the workpiece can be found as a function of the spring stiffness  $k_s$ , the free displacement of the actuator (without the spring)  $u_{2,free}$  and the displacement  $u_{2,unit}$  of the actuator subjected to a unit load  $p$  in the output direction

$$F_{out} = \frac{u_{2,free}}{u_{2,unit}/p + 1/k_s}, \quad (4)$$

where  $p$  is the unit load.

The force can be maximized by, in an optimal way, placing material in a subset  $\Omega_s$  of the design domain  $\Omega$ . The point-wise material distribution in the design domain is described by the relative density function  $\rho$ , where  $\rho$  takes the value 1 where there is material and 0 elsewhere. The optimization problem is now formulated as

$$\left. \begin{aligned} \max_{\rho} & F_{out}(\rho) \\ \text{s.t. :} & \int_{\Omega} \rho \, dx \leq V^* \\ & R(\rho) \geq R^* \\ & \rho(x) = 0 \text{ or } 1, \forall x \text{ in } \Omega \\ & \text{equilibrium equations} \end{aligned} \right\}, \quad (5)$$

where  $V^*$  is the upper bound on material volume and  $\mathbf{x}$  is the space coordinate.

## COMPUTATIONAL PROCEDURE

To solve the optimization problem (5) and the governing equations (1)-(3), the design domain is discretized using  $N$  4-noded finite elements. The relative density of material in each element  $e$  is  $\rho^e$ . The  $N$ -vector containing the design variables is denoted  $\rho$ . Since this 0-1 integer optimization problem is impossible to solve (it is a humongous combinatorial problem when  $N$  is large ( $> 5000$ )), the problem is modified to be a continuous one by allowing the design variables to take intermediate values. Converting the optimization problem to a continuous one, makes it possible to solve the problem with efficient mathematical programming methods making use of sensitivity analysis. For computational reasons (singularity of the stiffness matrix), the minimum value of the continuous design variables is not zero but takes a small value ( $\rho_{min} = 10^{-3}$ ). The discretized optimization problem can now be written as

$$\left. \begin{aligned} \max_{\rho} \quad & F_{out}(\rho) \\ \text{s.t. :} \quad & \sum_{e=1}^N \rho^e v^e \leq V^* \\ & R(\rho) \geq R^* \\ & 0 < \rho_{min} \leq \rho \leq 1 \\ & \text{equilibrium equations} \end{aligned} \right\}, \quad (6)$$

where  $v_e$  is the element volume.

The optimization problem (6) is non-linear and must be solved by an iterative procedure. The iterative optimization scheme used here is the method of moving asymptotes (MMA) suggested by Svanberg [7]. The MMA-scheme solves a sequence of linearized sub-problems and uses informations from prior iterations to improve convergence. The method is quite stable and computationally efficient and typically converges in a couple of hundred iterations.

The procedure is initiated by specifying material constants, boundary conditions, loadings, workpiece stiffness, geometry of design domain etc. Then the design domain is discretized by a large number of finite elements and the available material is distributed evenly throughout the domain. Now the iterations start. Each iteration consists in the following three steps: 1) solving three finite element problems for, respectively, the electric, the thermal and the elastic field; 2) performing an analytical sensitivity analysis (adjoint method) involving the solving of three extra load cases to the finite element problems and 3) doing an optimal material redistribution based on the MMA-scheme. The procedure has converged when the changes in design variables from iteration to iteration gets below a certain value (typically  $10^{-3}$ ). Usually less than 500 iterations are needed to converge to a good design. Depending on the number of elements and the complexity of the design domain, the

whole design process may take from a few minutes to a night on a powerful workstation. For simple or preliminary studies, however, the program can also be run on a laptop.

Different problems occur when solving the optimization problem as described. The problems which are described in the literature on topology optimization (e.g. [2] or in a recent review paper [8]) are occurrences of regions with alternating solid and void elements, referred to as checkerboards, and a strong mesh dependency of the solutions. Here, a mesh-independency algorithm suggested in [5] and [9] that both eliminates the checkerboard problem and the mesh-dependency problem is applied.

For more details on computational procedures, the reader is referred to the vast literature on topology optimization of structural systems or to [2] for an overview. For more details on the application of topology optimization to compliant mechanism design see [5].

## EXAMPLES

The devices considered here are all made from electroplated Nickel on Silicon wafers. Material properties of nickel (Ni) are: Young's modulus  $E^0 = 200$  GPa, thermal expansion coefficient  $\alpha = 13.4 \cdot 10^{-6}$  m/(m K), thermal conductivity  $k_1^0 = 90.7$  W/(K m), Poisson's ratio 0.31 and the electric conductivity is  $k_0^0 = 14.3 \cdot 10^6$  ( $\Omega\text{m}$ )<sup>-1</sup>. The thermal conductivity of air is  $k_{air} = 3.13$  W/(K m). The convection from the surfaces of the structure is governed by the Nusselt number which is dependent on Reynolds number, geometry and a characteristic length scale. For the small structure considered here, the Reynolds number is close to zero and therefore the Nusselt number can be estimated to be constant  $Nu = 0.36$ . A rather big simplification is made in assuming that the individual parts of the structure are horizontal cylinders with diameter given by the characteristic length scale  $D = 20\mu\text{m}$ . The convection coefficient from a surface can then be written as  $h = k_{air} Nu/D = 56 \cdot 10^3$  W/(m<sup>2</sup>K). For computational simplicity, the convection is assumed to happen only from the top surfaces. The simplifications of the convection process may seem rather crude, but considering how uncertain material properties of thin-film processed materials are, the simplification may drown in other uncertainties.

### "Conventional" actuator

As an example of design of an electrically actuated microactuator, the problem sketched in Fig. 3a is considered. The design domain is rectangular with dimensions  $500 \times 200 \mu\text{m}$  and thickness  $20 \mu\text{m}$ . The left edge has two terminals (shown in black) where a prescribed voltage of 0.25 volts is applied. A small rectangular domain

(shown in white) is fixed to be void. The optimization problem consists in maximizing the force exerted on a vertical spring of stiffness 600 N/m, which is attached to the structure at the center of the right edge.

A solution to this design problem is known from literature [10] and is shown in Fig. 3b. In the following, the electrothermal actuator in Fig. 3b will be referred to as the "conventional" actuator. The principle of actuation in the conventional actuator (Fig. 3b) is simple to explain. Due to higher resistance in the lower part of the actuator, the temperature here will increase more than in the top part due to resistive heating. Therefore the thin lower part will expand more than the top part and cause an upwards deflection. The work performed on the spring by the "conventional" actuator is 32 nJ and the resistance of the device is 0.14  $\Omega$ .

To see if a better design than the "conventional" actuator can be obtained, the topology optimization method is used to solve the same problem but now allowing the material to be distributed freely in the design domain. The "optimal" actuator is shown in Fig. 3c. It is seen that the optimal structure is almost short-circuited resulting in a large temperature increase near the terminals. Due to the temperature increase, the lower left part of the device expands and causes the right part of the structure to rotate upwards by a levering effect. The work performed on the spring is 84 nJ or almost 150% more than before but the resistance is very low - namely 0.013  $\Omega$ .

The very low resistance of the new design (Fig. 3c) is impractical and therefore a minimum constraint on the device resistance is imposed on the optimization problem. Constraining the resistance to be higher or equal to the resistance of the "conventional" actuator (Fig. 3b) the optimal actuator topology shown in Fig. 3d is obtained. The new design is seen to be very similar to the "conventional" design but the work performed on the spring is 54 nJ corresponding to a more than 60% improvement. The deflection at the output point is approximately 10  $\mu\text{m}$  and the force exerted on the spring is approximately 5.7 mN.

It should be mentioned that buckling is not considered in the FE-modelling of the devices at the present stage of development of the software. The actuators Fig. 3b and d both have problems with buckling. The buckling problem was discussed in [10] and also seen experimentally in the preliminary test of the devices designed here.

### "New" thermoelectric actuator

In the "conventional" actuator design problem in the previous example, the two terminals were placed on the left edge of the design domain. In this example the terminals are placed at each end of the device and the output point is at the center of the top edge as sketched

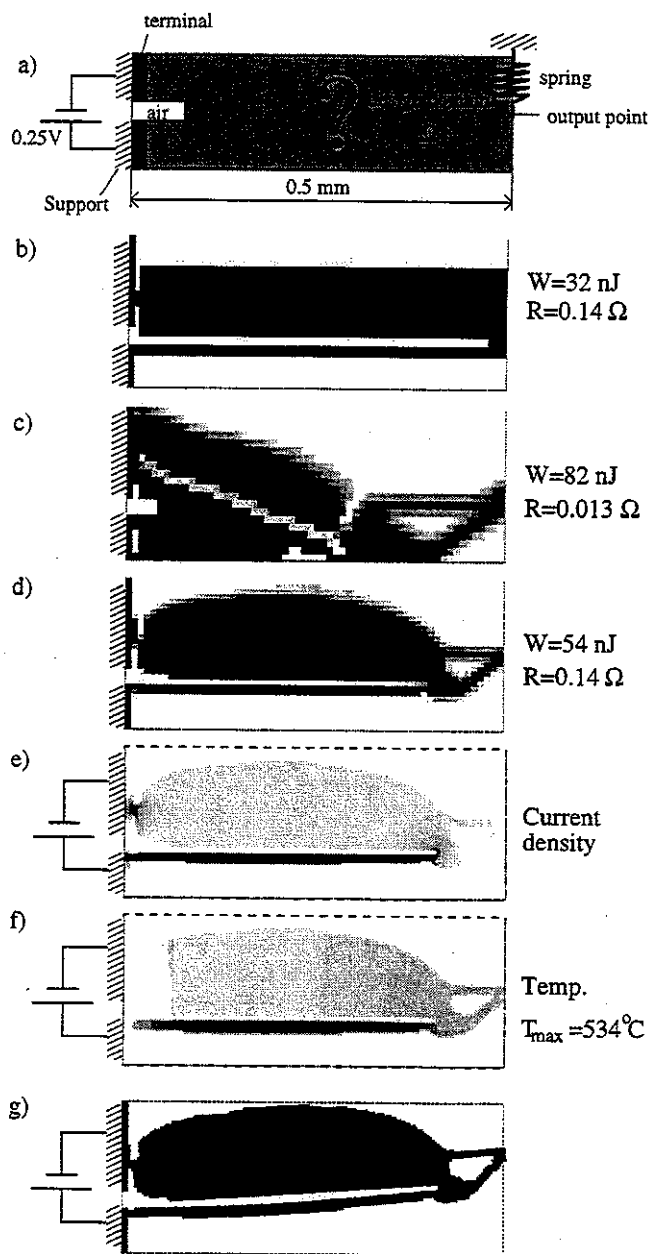


Figure 3: a: Definition of the electrothermomechanical actuator design problem. b: "Conventional" actuator topology known from literature [10]. c: Optimal actuator topology when resistance is not constrained ( $90 \times 30 = 2700$  elements). d: Optimal actuator topology when resistance is constrained ( $60 \times 20 = 1200$  elements). The grey scaling indicates intensity (white is zero and black is maximum). e: Plot of electric current density of design d. f: Plot of temperature distribution of design d. f: Displacement plot of design d.

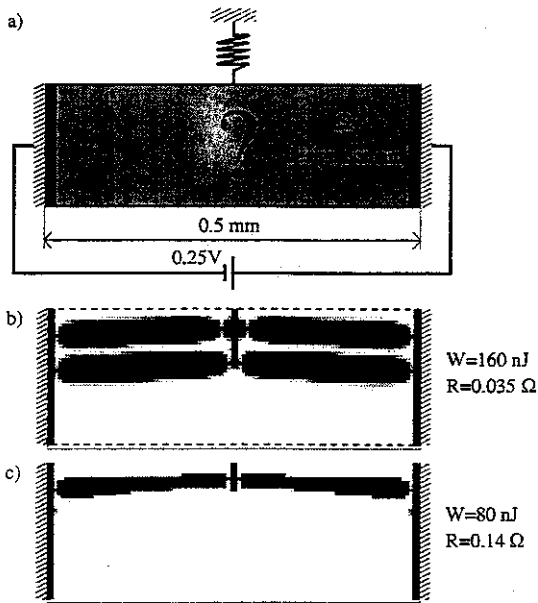


Figure 4: Electrothermomechanical actuator design problem with different terminal-placement. a: The design problem. b: Optimal design for free resistance. c: Optimal design for bounded resistance. The number of element in both designs is  $75 \times 30 = 2250$ .

in Fig. 4a.

The optimal topologies for, respectively, free minimum resistance and minimum resistance constrained to be that of the "conventional" design are shown in Figs. 4b and c. The output works of the two new designs are, respectively, 100% and 60% higher than those of Figs. 3c and d. Since the beam lengths in Figs. 4a and b are much shorter than those of Figs. 3c and d, the former will also be superior with respect to buckling. The output force of the actuator in Fig. 4b is 9.8 mN and the displacement is  $16 \mu\text{m}$ .

This example shows that not only the topology of the devices but also the placement of terminals greatly influences actuator performance.

### XY-scanning device

This example shows how actuators with multiple inputs and outputs can be designed using the topology optimization method as well. The design problem is sketched in Fig. 5a. The goal is to come up with a device that moves the output point (center right edge) horizontally when an electric field is applied to the left-most terminals and vertically when an electric field is applied on the rightmost terminals. At the same time there should be no cross-sensitivity between the outputs. To solve this design problem several new constraints are added to the original optimization problem from Eq. (6) and the extensions include the solving of six additional FE-problems. Due to the limited space these extensions will be discussed in more details elsewhere.

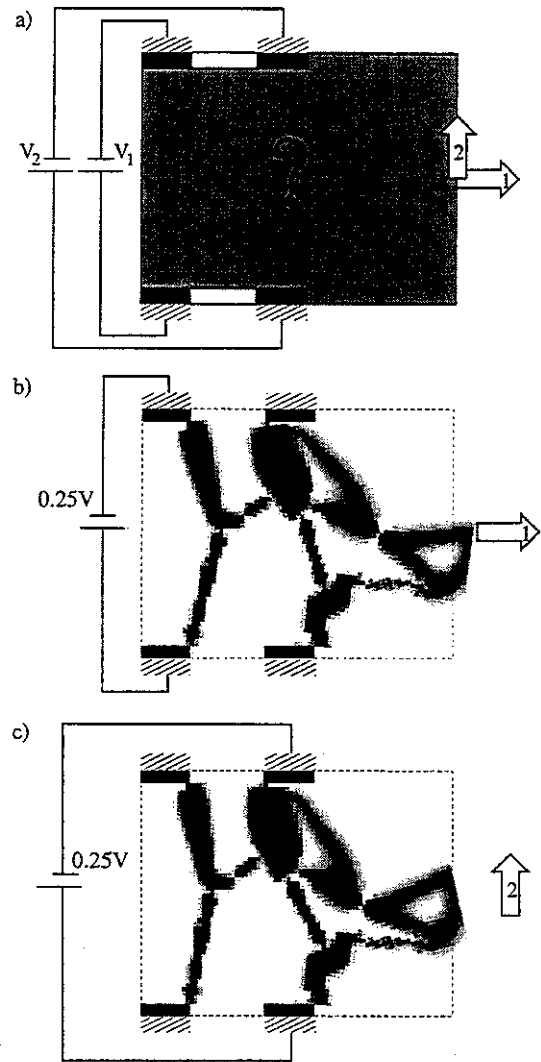


Figure 5: Design of xy-scanner where output points moves vertically for one electrical input and horizontally for another electrical input. a: Design problem. b: Horizontal displacement mode. c) Vertical displacement mode. The design domain is discretized by  $75 \times 60 = 4500$  elements.

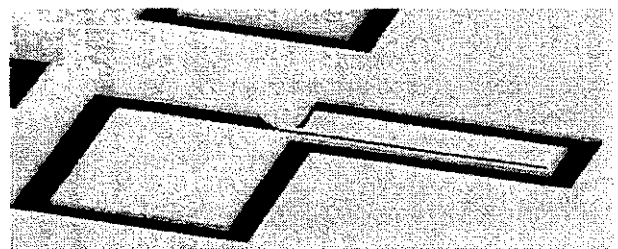


Figure 6: Micromachined thermal actuator fabricated by J. Jonsmann and S. Bouwstra at Mikroelektronik Centret, DTU, Denmark.

The optimal design subject to the two electrical inputs is shown in Fig. 5b and c. The optimal xy-scanning topology is seen to be rather complex but for the horizontal movement (input 1) the actuation happens mainly in the left part of the structure which is seen to resemble the optimal actuator from Fig 4c.

## MANUFACTURING

The thermal actuator can be manufactured using laser-micromachining as described for *passive* devices in [4]. The base material is electroplated Nickel on a silicon chip. A "conventional" thermoelectromechanical microactuator (Fig. 3b) has been manufactured at Mikroelektronik Centret, MIC at the Technical University of Denmark. The finished device is shown in Fig. 6. The performance of the actuator is presently being characterized together with the other devices designed in this article. Comparisons with predicted values will be presented elsewhere.

## CONCLUSIONS

A software for the optimal design of compliant electrothermal microactuators with high output force and complex output behaviour is being developed. At present, geometrical and material non-linearities and buckling behaviour of the devices are not considered. However these issues are subject to on-going research.

To obtain higher efficiencies of the actuators, the design problem can be extended to allow for two or more materials with different thermal expansion coefficients and void. This extension was done for the design of material microstructures with extreme thermal expansion coefficients [11]. For the electrothermal actuators, interesting possibilities arise if the two materials also have different electric conductivity. If one material is an insulator and the other a conductor, the electric field can be lead to the spot where actuation is needed.

Based on the findings of this paper and previous work on design of passive and active microactuators [5] and [6], it may be concluded that the topology optimization method is a promising tool for the systematic design of the mechanical parts and the electromechanical coupling parts of MicroElectroMechanical Systems.

## ACKNOWLEDGMENTS

The author is grateful to Krister Svanberg for supplying the MMA-optimization subroutines and to Martin P. Bendsøe, Pierre Duysinx, Pauli Pedersen and Daniel A. Tortorelli for many helpful discussions. The author also gratefully acknowledges the work of Jacques Jonsmann and Siebe Bouwstra at Mikroelektronik Centret (MIC), Technical University of Denmark, who produced the micromachined devices. The work presented in this pa-

per received support from the THOR-Program of Denmark's Technical Research Council (Design of MicroElectroMechanical Systems (MEMS)).

## REFERENCES

- [1] M. P. Bendsøe and N. Kikuchi. Generating optimal topologies in optimal design using a homogenization method. *Computational Methods in Applied Mechanics and Engineering*, 71:197-224, 1988.
- [2] M. P. Bendsøe. *Optimization of Structural Topology, Shape and Material*. Springer, 1995.
- [3] G. K. Ananthasuresh, S. Kota, and Y. Gianchandani. A methodical approach to the design of compliant micromechanisms. In *Solid-state sensor and actuator workshop*, pages 189-192, 1994.
- [4] U. D. Larsen, O. Sigmund, and S. Bouwstra. Design and fabrication of compliant mechanisms and material structures with negative Poisson's ratio. *Journal of Microelectromechanical Systems*, 6(2):99-106, June 1997.
- [5] O. Sigmund. On the design of compliant mechanisms using topology optimization. *Mechanics of Structures and Machines*, 25(4):495-526, November 1997.
- [6] O. Sigmund. Design of thermomechanical actuators using topology optimization. In W. Gutkowski and Z. Mroz, editors, *Second World Congress on Structural and Multidisciplinary Optimization, Zakopane, Poland, May*, pages 393-398. IFTR, 1997.
- [7] K. Svanberg. The method of moving asymptotes - a new method for structural optimization. *International Journal for Numerical Methods in Engineering*, 24:359-373, 1987.
- [8] O. Sigmund and J. Petersson. Checkerboards and mesh-dependencies in topology optimization. *To appear in Structural Optimization*, 1998.
- [9] O. Sigmund. *Design of material structures using topology optimization*. PhD thesis, Department of Solid Mechanics, Technical University of Denmark, December 1994.
- [10] J.H. Comtois and V. M. Bright. Thermal microactuators for surface-micromachining processes. In *Proceedings SPIE, vol. 2642*, pages 10-21, 1995.
- [11] O. Sigmund and S. Torquato. Design of materials with extreme thermal expansion using a three-phase topology optimization method. *Journal of the Mechanics and Physics of Solids*, 45(6):1037-1067, 1997.